Photochemistry and Photobiology, 2005, 81: 1075–1085

Symposium-in-Print: Ultraviolet Radiation and Terrestrial Ecosystems

Evaluating UV-B Effects and EDU Protection in Soybean Leaves Using Fluorescence

Elizabeth M. Middleton*[1], Moon S. Kim[2], Donald T. Krizek[3] and Ravinder K. S. Bajwa[4†]

[1]Biospheric Sciences Branch, NASA/Goddard Space Flight Center, Greenbelt, MD
[2]Instrumentation and Sensing Laboratory, Agricultural Research Service, USDA, Beltsville, MD
[3]Sustainable Agricultural Systems Laboratory, Agricultural Research Service, USDA, Beltsville, MD
[4]Department of Biology, Bergen County Academies, Hackensack, NJ

Received 25 April 2005; accepted 4 July 2005; published online 15 July 2005 DOI: 10.1562/2005-04-25-RA-498

ABSTRACT

A growth-chamber experiment was conducted to evaluate whether ethylenediurea (EDU), a chemical shown to be protective against ozone pollution, could ameliorate foliar damage induced by ultraviolet-B (UV-B) radiation exposure in 'Roanoke' soybean (*Glycine max* L.), a UV-B–sensitive cultivar, and whether these effects could be discriminated using fluorescence (F) observations. The experiment had four treatment groups: control; biologically effective UV-B (18 kJ m^{-2} day^{-1}); EDU (500 µmol mol^{-1}); and both UV-B and EDU (UV/EDU). Measurements included photosynthetic pigments, F image system (FIS) images of adaxial surfaces in four spectral regions (blue, green, red and far-red) and F emission spectra of the pigment extracts produced at two excitation wavelengths, 280 nm (280EX) and 380 nm (380EX). Several F ratios from 280EX, 380EX and the FIS images successfully separated the low UV *vs* high EDU group responses based on means alone, with intermediate values for controls and the combined UV/EDU groups. A UV-B/blue emission ratio, F315/F420 (280EX), was correlated with chlorophyll content (µg cm^{-2})($R = 0.88$, $P < 0.001$), as was a ratio of emissions at two UV-A wavelengths: F330/F385 (280EX) ($R = 0.87$). These two 280EX ratios were also linearly correlated with emission ratios produced by 380EX, such as the far-red/green ratio, F730/F525 (380EX) ($R = 0.92$, $P < 0.001$), and clearly distinguished the UV-B and EDU groups separately, and which bracketed the similar intermediate responses of the UV/EDU and control groups. The FIS images additionally captured the following anatomical spatial patterns across the leaf surfaces: (1) emissions of UV-B–irradiated leaves were more uniform but lower in intensity than those of other groups; and (2) emissions of EDU-treated leaves exhibited the greatest variation in spatial patterns because veins had elevated blue F and leaf edges had enhanced red and far-red F. This experiment supports the hypothesis that EDU substantially ameliorated UV-B damage to foliage, a result that relied on the combined use of FIS images and emission spectra.

INTRODUCTION

Ultraviolet-B (UV-B, 280–320 nm) irradiation damage to vegetation is well documented (1). The most common responses to long-term UV-B exposure over a growing season are reduced photosynthetic pigment content and photosynthetic capacity, altered root-to-shoot ratios and altered foliage characteristics, which together lead to reduced leaf area, plant height and biomass. Protective mechanisms also develop (2–4), such as a thicker epidermis, accumulation of flavonoids (UV-B absorbing compounds) and hydroxycinnamic acids and a more lateral growth pattern. For short-term exposures, as in growth-chamber experiments, photosynthetic dysfunction may develop but changes in pigment content are inconsistent; a typical early protective response can be an increase in photosynthetic pigments (4–6). A means to ameliorate the potentially harmful exposures of spring and summer UV-B irradiation levels experienced by low- and mid-latitude crops could have economic benefits to producers. Ethylenediurea (EDU) is a compound successfully used in a soil drench on crops to ameliorate ozone damage (7–9). An earlier study found that soil uptake of EDU partially ameliorated UV-B exposures in cucumber, a sensitive crop (10). That study also examined the use of fluorescence (F) emission spectra and multiband F images in detecting foliage responses to UV-B and EDU. Chlorophyll fluorescence (ChlF) has been used for decades to evaluate photosynthetic function (11–14). F images (15–17) and spectra (18–24) have been used successfully to detect physiological status. F has also been used to investigate plant UV-B stress (10,25–28).

Given the protective role of EDU against UV-B–induced damage in our previous cucumber study (10), we extended our research to examine UV-B exposure and EDU uptake in a UV-B–sensitive soybean cultivar. In the current study, we con-

† Formerly at Troy State University, Troy, AL

* To whom correspondence should be addressed: Biospheric Sciences Branch (Code 614.4), NASA/Goddard Space Flight Center, Greenbelt, MD 20771 USA. Fax: 301-614-6695; e-mail: Elizabeth.M.Middleton@nasa.gov

Abbreviations: 280EX, fluorescence excitation wavelength at 280 nm; 380EX, fluorescence excitation wavelength at 380 nm; ChlF, chlorophyll fluorescence; DMSO, dimethyl sulfoxide; EDU, ethylenediurea; F, fluorescence; FIS, fluorescence imaging system; GLM, global linear model; HPS, high-pressure sodium; LPS, low-pressure sodium; MH, metal halide; PAR, photosynthetically active radiation; RFI, relative fluorescence intensity; UV-B, ultraviolet-B; $UV\text{-}B_{BE}$, biologically effective UV-B.

ducted a set of two experiments in sequence to evaluate the following: (1) whether EDU could provide protection against UV-B radiation; (2) whether UV-B and EDU effects could be discriminated using F spectral observations; (3) whether similar or different information was expressed by F spectra *vs* F images of leaves provided with EDU and UV-B exposure; and (4) whether the age of leaves influenced the F properties observed.

MATERIALS AND METHODS

Plant material and treatments

Two replicated factorial experiments (Exp. 1, Exp. 2) were conducted in July 1996 with four treatment groups: control (no UV, no EDU); EDU; UV-B; and UV-B and EDU together (UV/EDU). Five plants per treatment were included in each experiment (n = 40). The UV-B irradiation levels were equal in the two experiments. 'Roanoke' soybean (*Glycine max* L.) was used as experimental plant material because it was found previously to be sensitive to elevated UV-B radiation (Krizek 1992, unpublished results). Plants were grown in 12.7 cm diameter plastic pots containing 200 g of peat–vermiculite mix (Jiffy Mix, Jiffy Products of America, West Chicago, IL), fertilized daily with a complete nutrient solution, as described by Silvius *et al*. (29), and thinned to one plant per pot 4 days after germination.

At the time of full cotyledon expansion (after about 7 days), plants were given a soil drench of EDU at either 0 or 500 μmol mol^{-1} on 15 July (Exp. 1) and 22 July (Exp. 2). Plants were then placed in a growth chamber for 2 weeks under the following environmental conditions: 27°C day/night temperature, 50% relative humidity and 350 μmol mol^{-1} CO_2. The chamber contained an equal mix of 400W high-pressure sodium (HPS) and 400W metal halide (MH) lamps which provided 840 μmol m^{-2} s^{-1} photosynthetically active radiation (PAR, 400–700 nm) over a 12 h photoperiod (between 0730 and 1930 h), with 270 μmol m^{-2} s^{-1} provided for a 1 h transition period immediately before and after the photoperiod (0630–0730 h and 1930–2030 h).

Subsequently, the plants were transferred for UV treatment to a separate growth chamber containing 180W low-pressure sodium (LPS) lamps (Phillips North America, Bloomfield, NJ) to provide background PAR for 14 h (0630–2030 h) as well as supplemental UV irradiation as described below. The UV exposure chamber was maintained at the same temperature, relative humidity and CO_2 concentration as the HPS/MH growth chamber. The LPS chamber was divided into two compartments by a vertical sheet of UV-B–absorbing polyester film. UV-B 313 fluorescent lamps (Q-Panel Lab Products, Cleveland, OH) were mounted horizontally at ~0.5 m above the plants in both compartments. The lamps over the ''no UV'' compartment were wrapped with polyester (0.13 mm thick) to block UV-B irradiation, and those over the ''UV'' compartment were wrapped with cellulose diacetate (0.08 mm) to transmit UV-B radiation. The plants in these two compartments were exposed to either 0.2 or 18 kJ m^{-2} day^{-1} of biologically effective UV-B ($UV\text{-}B_{BE}$) radiation, normalized to unity for an 8 h period in the center of the 14 h photoperiod. The UV-B exposures were continued for 10 days. UV-B irradiance at plant level was monitored with a portable UV radiometer (Minimum Erythemal Dose, MED Meter, Solar Light Co., Philadelphia, PA), calibrated with a UV spectroradiometer (model 752, Optronics Laboratory, Inc., Orlando, FL), and adjustments were made to maintain constant exposure levels. Following UV-B irradiation, plants were returned to the HPS/MH growth chamber.

The treatments are summarized: (1) control plants (0.2 kJ $UV\text{-}B_{BE}$ m^{-2} day^{-1}, no EDU); (2) UV-B–exposed plants (18 kJ $UV\text{-}B_{BE}$ m^{-2} day^{-1}, no EDU); (3) EDU-exposed plants (0.2 kJ $UV\text{-}B_{BE}$ m^{-2} day^{-1}, 500 μmol mol^{-1} EDU); and (4) plants provided combined UV-B and EDU exposures (18 kJ $UV\text{-}B_{BE}$ m^{-2} day^{-1}, 500 μmol mol^{-1} EDU). Two experiments were conducted in sequence in 1996, each with 10 days of UV-B irradiation and EDU uptake (after a single EDU application).

Measurements

After 10 days of UV-B irradiation and EDU uptake, measurements in both experiments were made of pigment content and spectral F emissions, on both the oldest (unifoliate) leaf and the youngest fully expanded trifoliate leaf per plant.

Multispectral fluorescence images. A custom F imaging system (FIS) was used to acquire steady-state F emission images of whole leaves or leaflets in four spectral bands (30). The band regions, with their center wavelengths and full widths at half-maximum were the blue (450, 25 nm), green (550, 25 nm), red (680, 10 nm) and far-red (740, 10 nm). Emissions in these bands were actively induced by a broadband (300–400 nm) UV excitation source consisting of four 15W long-wave UV-A lamps with peak output centered at 365 nm (UV-A fluorescent lamps, model EA-180/12, Spectroline Inc., Westbury, New York) filtered with Schott UG-1 glass to eliminate radiation >400 nm. The lamps were arranged at a 45° angle toward a central target area approximately 0.2 m above the sample surface to provide nearly uniform broadband illumination with an intensity of 0.33 mW cm^{-2}. The FIS consists of a thermoelectrically cooled digital camera and optics (Lynxx-2 charge coupled device [CCD] camera; Spectra Source Instruments, Westlake Village, CA), a motorized filter wheel (CVI Inc., Albuquerque, NM) and a desktop computer interface for data storage and instrument control. A horizontal surface painted nonfluorescent flat black served as the platform for leaf samples, situated ~0.5 m below the down-looking CCD camera.

Freshly excised leaves were placed on the platform with adaxial surfaces upward to be viewed by the CCD. For each image, four leaves (or central leaflets of trifoliate leaves) were placed in a fixed arrangement on the platform (*e.g*. replicate #2 of each treatment group), one per treatment arranged clockwise from the upper left corner in this order: control, UV, UV/EDU, EDU. Nonsaturated images were acquired in each of the four spectral bands for each replicated set. A simple threshold method was used to create a masked image of leaves in each spectral band, within which F means and standard deviations (SD) for masked regions of each of the individual leaves were determined using image processing software developed in MS Windows (Visual Basic V. 6.0, Microsoft Corp., Redmond, WA). Images were also produced for ''regions of interest'' to enhance the spatial F patterns across the adaxial lamina that resulted from localized treatment effects. Leaf surface regions expressing emissions similar to those of the control, UV and EDU groups were calculated and mapped as those regions exhibiting emissions within the ~99th percentile of the intensity histogram, per treatment mean. The percent coefficient of variation (CV) per treatment was computed ([SD ÷ mean] × 100) for FIS emissions of trifoliates from Exp. 2 to capture spatial variation across the leaf surface in each band.

Photosynthetic pigments and UV-B–absorbing compounds. Immediately following the FIS acquisitions, two leaf disks (1 cm diameter) were removed from the distal portion of these leaves for extraction of photosynthetic pigments (27). The disks were extracted in 4 mL dimethyl sulfoxide (DMSO) and kept for 24 h in the dark. Samples of the pigment extracts were placed in standard quartz cuvettes and analyzed in a computerized dual beam spectrophotometer (Lambda 3B, UV/VIS, Perkin-Elmer, Norwalk, CT). The absorption spectra were scanned at 1 nm resolution from 400 to 750 nm and used in equations described by Wellburn *et al*. (31) to calculate concentrations of photosynthetic pigments expressed on a per area basis (μg cm^{-2}), as also discussed by Barnes *et al*. (32).

An additional four leaf disks (1 cm diameter) were removed from the distal portion of each leaf for extraction of UV-B–absorbing compounds in ethanol acidified with glacial acetic acid (vol:vol, ethanol:acetic acid, 99:1). The disks were boiled gently for 10 min in a water bath at 80°C, and absorbances were read at 270, 300, and 330 nm (A270, A300, A330) using a UV-Visible Recording Spectrophotometer (UV-160A, Shimadzu, Columbia, MD) to assess relative concentrations of UV-absorbing compounds.

Fluorescence emission spectra. The DMSO pigment extracts were used for determination of F emission spectra (10,27). To prevent saturation of emission values, 20 μL of each leaf extract was diluted with DMSO and the total volume was brought to 4 mL in a quartz cuvette. A spectrofluorometer (Fluorolog II, SPEX Industries, Inc., Edison, NJ) with two double monochrometers attached to a 450 W xenon lamp was used to induce and collect steady-state F emission spectra from the leaf extracts. Fluorescence kinetics were not investigated. Emission spectra were obtained by stepping from shorter to longer wavelengths at 5 nm increments, after setting the excitation at fixed wavelengths of 280 or 380 nm (280EX, 380EX). For each sample, two F emission spectra were obtained: 280EX produced F between 300–600 nm and 380EX produced F between 400–800 nm. F responses were examined as a function of treatment group for full emission spectra (280EX and 380EX) and for individual emission values at selected wavelengths which represent F maxima, minima, or others features of interest. Emissions at these selected wavelengths are designated in a standard format: for example, $F675_{380EX}$ represents F at 675 nm resulting from excitation at 380 nm. Ratios of emissions at selected wavelengths were computed.

Data processing and statistical analysis. Each of the two experiments was conducted as a 2 × 2 × 2 factorial, with two levels of UV-B irradiation (0.2 and 18 kJ m^{-2} s^{-1}), two levels of EDU (0 and 500 μmol^{-1}), and 2 leaf types, replicated in two experiments (n = 80). Data from all groups were

Table 1. UV-B and EDU effects on photosynthetic pigments*, Means†, and standard errors (SE) by experiment, treatment group and leaf type

			Chlorophyll *a*		Chlorophyll *b*		Carotenoids		Ratio, Chl/carotenoid		Total pigment		Ratio, Chl *a*/Chl *b*	
Leaf type	Date	Treatment	Mean	± SE	Mean	± SE	Mean	± SE	Mean	± SE	Mean	± SE	Mean	± SE
Unifoliate	Exp. 1	Control	20.18_a	0.43	9.19_a	0.21	3.03_a	0.05	9.71_b	0.16	32.40_a	0.59	2.20_d	0.01
Unifoliate	Exp. 1	EDU	20.24_a	0.43	9.39_a	0.21	3.28_b	0.05	9.04_b	0.16	32.92_a	0.68	2.16_c	0.01
Unifoliate	Exp. 1	UV	21.43_b	0.43	10.12_b	0.21	3.21_b	0.05	9.83_a	0.16	34.76_b	0.51	2.12_b	0.01
Unifoliate	Exp. 1	UV/EDU	21.71_b	0.43	10.75_b	0.24	3.56_c	0.05	9.02_a	0.16	35.67_b	1.03	2.06_a	0.02
Trifoliate	Exp. 1	Control	20.35_a	0.42	8.84_a	0.31	3.20_a	0.07	9.13_b	0.09	32.38_a	0.84	2.31_b	0.03
Trifoliate	Exp. 1	EDU	20.77_a	0.42	9.00_a	0.31	3.44_b	0.07	8.87_a	0.11	33.21_a	0.70	2.27_b	0.03
Trifoliate	Exp. 1	UV	21.87_b	0.42	10.09_b	0.31	3.40_b	0.07	9.39_c	0.09	35.36_b	0.89	2.17_a	0.03
Trifoliate	Exp. 1	UV/EDU	22.97_c	0.42	10.62_b	0.31	3.70_c	0.07	9.09_b	0.09	37.28_c	0.47	2.17_a	0.03
Unifoliate	Exp. 2	Control	14.79_a	0.56	6.59_{ab}	0.25	2.21_a	0.10	9.68_b	0.15	23.59_a	0.88	2.25_{ab}	0.03
Unifoliate	Exp. 2	EDU	14.29_a	0.56	6.18_a	0.25	2.18_a	0.10	9.39_a	0.15	22.66_a	0.65	2.32_b	0.03
Unifoliate	Exp. 2	UV	15.86_a	0.56	7.05_b	0.25	2.38_b	0.10	9.67_{ab}	0.15	25.28_b	0.87	2.25_{ab}	0.03
Unifoliate	Exp. 2	UV/EDU	15.91_a	0.56	7.09_b	0.25	2.42_b	0.10	9.39_a	0.15	25.86_b	1.24	2.20_a	0.04
Trifoliate	Exp. 2	Control	8.72_a	0.50	3.39_a	0.21	1.56_a	0.08	7.76_a	0.27	14.12_a	0.75	2.56_b	0.05
Trifoliate	Exp. 2	EDU	8.61_a	0.50	3.36_a	0.18	1.57_a	0.07	7.61_a	0.24	13.55_a	0.64	2.56_b	0.05
Trifoliate	Exp. 2	UV	10.78_b	0.50	4.33_b	0.18	1.83_b	0.07	8.26_b	0.24	16.95_b	0.84	2.49_{ab}	0.05
Trifoliate	Exp. 2	UV/EDU	10.50_b	0.50	4.24_b	0.18	1.80_b	0.07	8.19_b	0.24	16.53_b	0.82	2.48_a	0.05

* Pigment contents are reported in μg cm^{-2}.
† Statistically different means are indicated by different letter subscripts.

incorporated into a summary spreadsheet for statistical analysis; means and standard errors (SE) were determined for all measurements. Significant differences among group means were determined using the Tukey–Kramer pairwise mean comparison test. Relationships among spectral variables were examined. A global linear model (GLM) analysis was performed on the combined data set with four main factors: UV-B (0, 1), EDU (0, 1), leaf type (trifoliate, unifoliate), and experiment (1, 2) with 2- and 3-factor interaction terms included (Systat Software V. 9.0, SPSS, Chicago, IL). Plots were produced with SigmaPlot (Systat Software, Inc., Point Richmond, CA, USA).

RESULTS

Leaf characters

The leaf pigment, dry mass and related variables are summarized in Tables 1 and 2. Chl *a*, Chl *b* and carotenoid content increased under UV-B exposure in both experiments. Because Chl *b* increases (+10%) were relatively greater than those for Chl *a* (+4%), Chl *a*/*b* ratios were lowered. The effect of UV-B treatment on total leaf UV-B–absorbing compounds as estimated by UV-B absorbances (*e.g.* A300) was inconsistent, with the only significant increase occurring in trifoliate leaves in Exp. 1. In general, leaf area was reduced by UV-B exposure, and leaf dry weight was lowered by either EDU uptake or UV-B exposure.

Fluorescence of extracts

The mean F emissions of leaf extracts produced from 280EX and 380EX are shown in Figs. 1a and 1b, respectively, for trifoliate leaves. From 280EX, emission spectra separated according to treatment in the broad protein peak between 315–350 nm, with the highest F produced by EDU plants and the lowest from UV plants;

Table 2. UV-B and EDU effects on selected leaf parameters: Means* and standard errors (SE) by experiment, treatment group and leaf type

			A300 nm (Abs cm^{-2})		Leaf area (cm^2)		Leaf fresh wt. (g)		Leaf dry wt. (g)		SLA† (cm^2 g^{-1})	
Leaf type	Date	Treatment	Mean	± SE	Mean	± SE	Mean	± SE	Mean	± SE	Mean	± SE
Unifoliate	Exp. 1	Control	0.37_b	0.03	19.72_a	1.72	0.406_a	0.027	0.0570_b	0.004	353.0_a	37.9
Unifoliate	Exp. 1	EDU	0.39_b	0.03	20.49_a	1.72	0.374_a	0.027	0.0430_a	0.004	494.0_c	53.2
Unifoliate	Exp. 1	UV	0.30_a	0.03	18.74_a	1.72	0.376_a	0.027	0.0600_b	0.004	321.8_a	39.7
Unifoliate	Exp. 1	UV/EDU	0.34_{ab}	0.03	20.91_a	1.72	0.446_a	0.027	0.0490_a	0.004	430.2_b	12.3
Trifoliate	Exp. 1	Control	0.35_b	0.01	21.62_b	1.38	0.297_{ab}	0.032	0.0300_b	0.003	659.7_b	30.7
Trifoliate	Exp. 1	EDU	0.29_a	0.01	22.04_b	1.50	0.314_b	0.034	0.0250_a	0.003	941.9_b	102.3
Trifoliate	Exp. 1	UV	0.38_c	0.01	16.37_a	1.67	0.230_a	0.026	0.0340_b	0.003	497.5_a	86.9
Trifoliate	Exp. 1	UV/EDU	0.40_c	0.01	15.77_a	0.70	0.224_a	0.023	0.0230_a	0.003	693.4_b	41.7
Unifoliate	Exp. 2	Control	0.40_c	0.01	27.14_b	1.12	0.448_b	0.035	0.0610_{ab}	0.004	446.3_b	29.6
Unifoliate	Exp. 2	EDU	0.37_c	0.01	26.46_b	1.12	0.480_c	0.035	0.0590_a	0.004	449.12_b	23.3
Unifoliate	Exp. 2	UV	0.26_b	0.01	21.10_a	1.12	0.360_a	0.035	0.0550_a	0.004	388.20_a	22.9
Unifoliate	Exp. 2	UV/EDU	0.22_a	0.01	22.81_a	1.12	0.394_a	0.035	0.0660_b	0.004	354.6_a	34.6
Trifoliate	Exp. 2	Control	0.39_c	0.01	23.44_c	1.67	0.430_a	0.031	0.0720_b	0.004	335.4_a	40.6
Trifoliate	Exp. 2	EDU	0.38_c	0.01	21.55_b	0.91	0.394_a	0.026	0.0630_a	0.004	348.0_a	28.2
Trifoliate	Exp. 2	UV	0.26_b	0.01	21.87_b	1.09	0.405_a	0.025	0.0600_a	0.004	378.5_a	42.8
Trifoliate	Exp. 2	UV/EDU	0.23_a	0.01	20.97_a	1.09	0.394_a	0.025	0.0610_a	0.005	349.9_a	31.8

* Statistically different means are indicated by different letter subscripts.
† Specific leaf area.

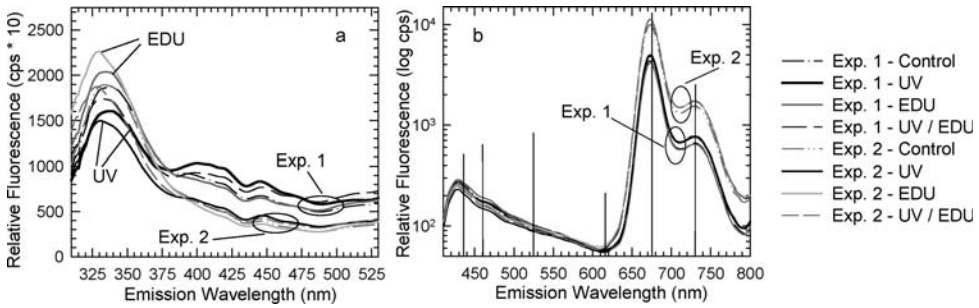

Figure 1. The emission spectra produced from DMSO extracts from trifoliate leaves are shown for the four treatments (control, UV, EDU, UV/EDU) in two experiments (Exps. 1 and 2) for **a**] 280EX and **b**] 380EX. Emission wavelengths (315, 330, 385, 420 and 445 nm) found to give significant treatment separations are indicated by vertical lines in panel b].

emissions for the combined UV/EDU treatment and the controls were intermediate. However, F emissions between 380–530 nm clustered by experiment (Exp. 1 > Exp. 2) rather than by treatment. From 380EX, the emissions were similar for all groups between 400–610 nm, beyond which the spectra clustered by experiment (Exp. 2 > Exp. 1) in the red and far-red ChlF regions. For both 280EX and 380EX, the separation by experiment was more pronounced for trifoliates than for unifoliates (spectra not shown).

All 16 groups (four treatments, two experiments, two leaf types) were further examined at select F wavelengths and in the major UV peak of 280EX emission spectra, highlighting the finding that EDU treatment enhanced UV-A fluorescence whereas UV treatment reduced it. The F emission variables that produced the strongest treatment differences are shown in Fig. 2 (a–d). For F at 315 nm ($F315_{280EX}$; Fig. 2a) and a UV ratio of $F330/F385_{280EX}$ (Fig. 2b) treatment effects were strongly expressed overall, in spite of significant differences due to experimental replication and leaf age (*i.e.* significant differences among the four bars per treatment). The pattern of response obtained was that EDU enhanced, but UV-B depressed, F emissions, producing the highest and lowest group values, respectively. The combined UV/EDU treatment groups produced intermediate values that were similar to (or overlapped) those of the control groups. This pattern was accentuated by using a ratio of emissions at the 330 nm UV-A peak normalized to the local UV-A minimum at 385 nm, or $F330/F385_{280EX}$ (Fig. 2b), but this also accentuated the differences due to experimental replication (Exp. 2 > Exp. 1). Another ratio, $F330/F445_{280EX}$, which comprised F330 and emissions at the 445 nm, clearly distinguished young from old leaves (Fig. 2c) and maintained this same general response pattern among treatments. In all of these responses, both the UV and EDU treatments influenced the observed F intensities or F ratios. There was only one 280EX variable for which EDU produced a significant main effect, by lowering the blue/green $F435/F525_{280EX}$ ratios (Fig. 2d).

The responses to treatments were not as clearly defined with emissions produced by 380EX (Fig. 3a, 3b). An augmentation in ChlF was only seen when expressed as a ratio, such as with the red/blue ratio of $F675/F460_{380EX}$ (Fig. 3a) or the far-red/green (380EX) ratio (not shown), which produced similar trends. Otherwise, no generalized pattern for treatment effects could be observed in the ChlF region, as shown by a ratio that normalizes maximum ChlF emissions at 730 nm (or 675 nm, not shown) to the

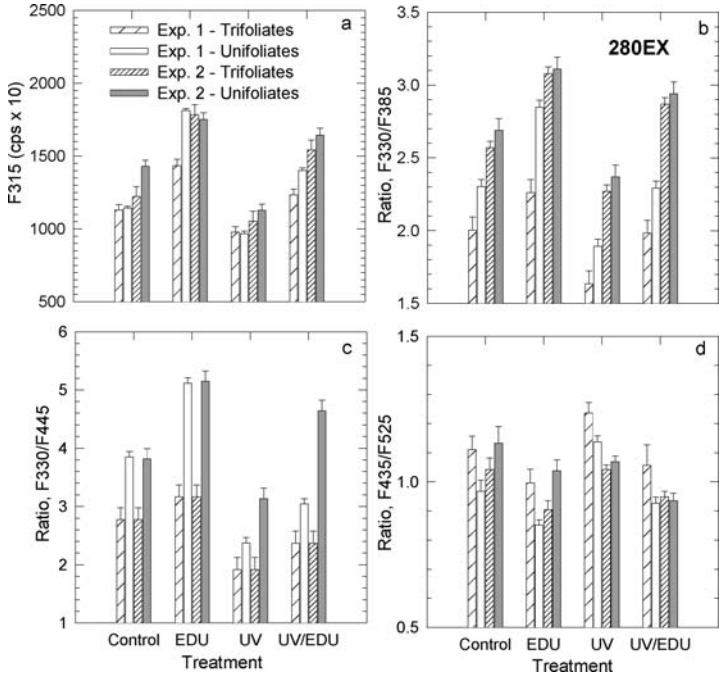

Figure 2. Bar charts show the mean ± SE of four 280EX fluorescence variables of DMSO extracts, for the 16 plant groups included in this study. These are arranged by the four treatments (control, EDU, UV and UV/EDU). Also shown are four other groups: trifoliates from Exp. 1, hatch; trifoliates from Exp. 2, dense hatch; unifoliates from Exp. 1, white; and unifoliates from Exp. 2, grey. The four 280EX F emission variables are **a**] F315; **b**] the F330/F385 ratio; **c**] the F330/F445 ratio; and **d**] the F435/F525 ratio.

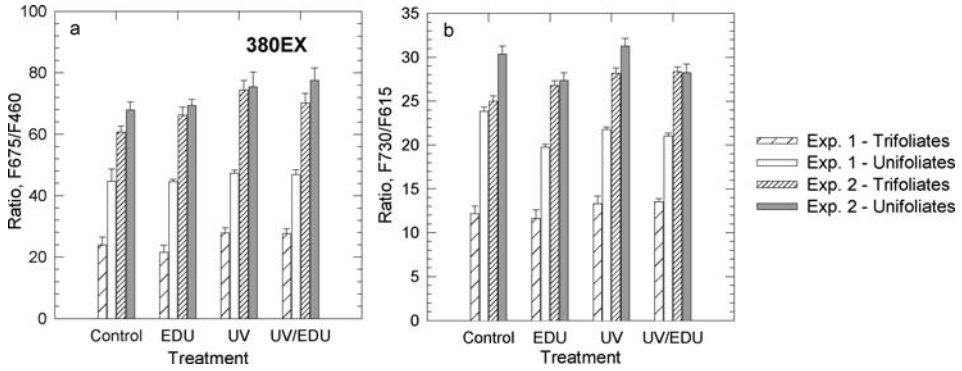

Figure 3. Bar charts show the mean ± SE of two 380EX fluorescence ratios of DMSO extracts, for the 16 plant groups included in this study. These are arranged by the four treatments (control, EDU, UV and UV/EDU). Also shown are four other groups: trifoliates from Exp. 1, hatch; trifoliates from Exp. 2, dense hatch; unifoliates from Exp. 1, white; and unifoliates from Exp. 2, grey. The two 380EX F emission variables are **a**] the F675/F460 ratio and **b**] the F730/F615 ratio.

minimum at 615 nm, or $F730/F615_{380EX}$ (Fig. 3b). Nevertheless, three of the four groups receiving UV-B exposures (UV and UV/EDU) were distinguished from the EDU and control groups.

The four treatments, when combined over experiments and leaf types, were clearly defined by linear correlations of a 280EX ratio ($F330/F385_{280EX}$) to 380EX ratios: either a $ChlF/blue_{380EX}$ ratio ($F730/F435_{380EX}$, $R = 0.92$, Fig. 4) or a ChlF/green ratio ($F675/F525_{380EX}$, $R = 0.90$, data not shown). This approach offers a method for detecting leaves from UV *vs* EDU treatments, and preserves the pattern already described above of enhanced EDU and quenched UV, relative to the intermediate and overlapping relationships for controls and the combined UV/EDU treatment.

Fluorescence images

First, it must be stated that there were no visible differences among leaves that could be attributed to the experimental treatments. However, responses to treatments were apparent in the FIS images, which conveyed considerable information about the strength and spatial distribution of F intensities, thus indicating complex physiological responses, as shown for the center leaflets of trifoliates in Fig. 5 (a–d) and Fig. 6 (a–c). Consistent treatment responses were not obtained with the green band images (Fig. 5b). However, a response pattern similar to that described above for 280EX emissions of extracts is immediately apparent in the ChlF images in the red_{FIS} and $far\text{-}red_{FIS}$ bands (Fig. 5c,d): augmented F in EDU leaves, reduced F in UV-B leaves and intermediate F in the combined UV/EDU treatment and in controls. This response pattern was further highlighted in the $far\text{-}red_{FIS}$ and the $far\text{-}red/blue_{FIS}$ images (Figs. 6b,c). In the $blue_{FIS}$ images (Fig. 6a), UV-B–exposed leaves (UV, UV/EDU) were discriminated from others by lower F.

The FIS images also provided spatial information (*e.g.* localized treatment effects) across the adaxial leaf surfaces, expressed as

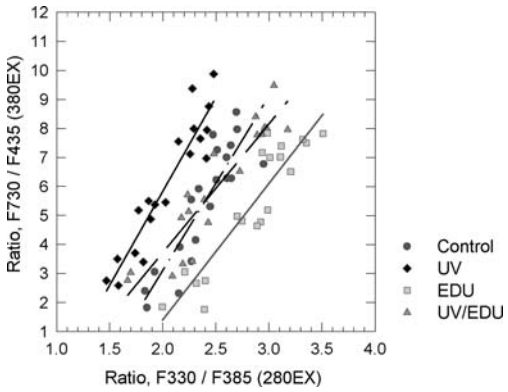

Figure 4. A 380EX far-red/blue F ratio (F730/435) and a 280EX UV-A F ratio (F330/F385) are linearly correlated ($R = 0.92$, $n = 80$) and successfully discriminate the EDU- and UV-exposed foliage at opposite ends of the 280EX ratio's range, with intermediate values for the control and UV/EDU groups. Separate linear relationships are shown for the four treatments (control, dark grey circles; UV, black diamonds; EDU, light grey squares; and UV/EDU, medium grey triangles). Treatments include all available data for both leaf types and both experiments.

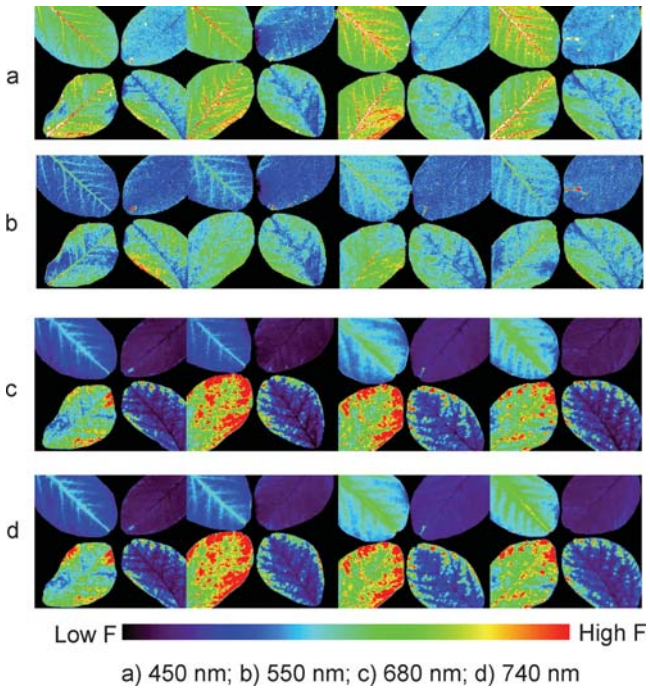

Figure 5. FIS images are shown for four replicates (left to right) in each of the four bands (**a–d**) stacked vertically: $blue_{FIS}$, $green_{FIS}$, red_{FIS} and $far\text{-}red_{FIS}$. Each of the 16 figure sectors displays the adaxial surface F of leaflets arranged by treatment. In each sector, leaflets are arranged clockwise from the upper left corner (control, UV, UV/EDU and EDU). The same leaflet is shown in the four bands vertically (top to bottom, a–d), with four of the five available replicates displayed in the four columns (left to right). The colors describe the relative F intensity, as given by the color bar at the bottom, where purple indicates low F and red indicates high F.

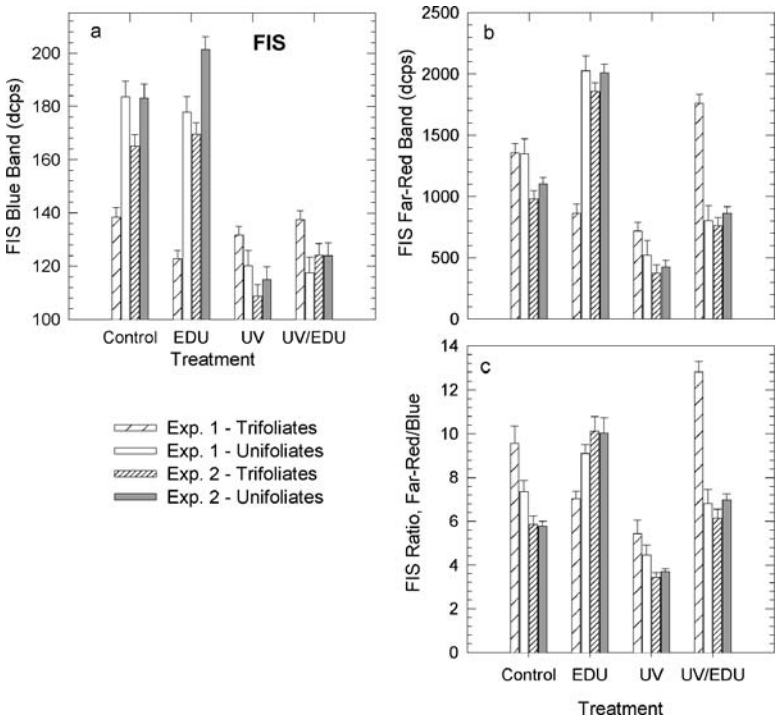

Figure 6. Bar charts show the mean ± SE for three FIS images for the 16 plant groups included in this study. These are arranged by the four treatments (control, EDU, UV and UV/EDU). Also shown are four other groups: trifoliates from Exp. 1, hatch; trifoliates from Exp. 2, dense hatch; unifoliates from Exp. 1, white; and unifoliates from Exp. 2, grey. The three FIS variables are: **a**] the FIS blue band, $blue_{FIS}$; **b**] the FIS far-red band, $far\text{-}red_{FIS}$; and **c**] the $far\text{-}red/blue_{FIS}$ ratio.

variation in emission intensities. From the red band images presented in Fig. 5c, regions of similarity (Fig. 7) indicate that leaf intervenous regions in the combined UV/EDU treatment were similar in F intensity to controls (Fig. 7, top panel) but that the F of venous regions for the combined UV/EDU treatment were similar to UV leaves (Fig. 7, middle panel). No other leaf regions were similar to the high ChlF intensity of EDU leaves, except for small spots along the leaf edges of UV/EDU leaves (Fig. 7, bottom panel). The spatial patterns and F intensities across the surfaces of control *vs* UV leaves contrasted greatly, as for $green_{FIS}$ F of the central trifoliate leaflet (Fig. 8). UV-exposed leaves had more spatially uniform $blue_{FIS}$ F (CV = 18 ± 3%) than did control leaves (CV = 28 ± 5%). The ChlF bands captured the greater spatial heterogeneity of the UV/EDU leaves (red_{FIS} band, CV = 65 ± 3%; $far\text{-}red_{FIS}$, CV = 52 ± 4%) as compared to the controls (CV = 18–23 ± 3%, both ChlF bands).

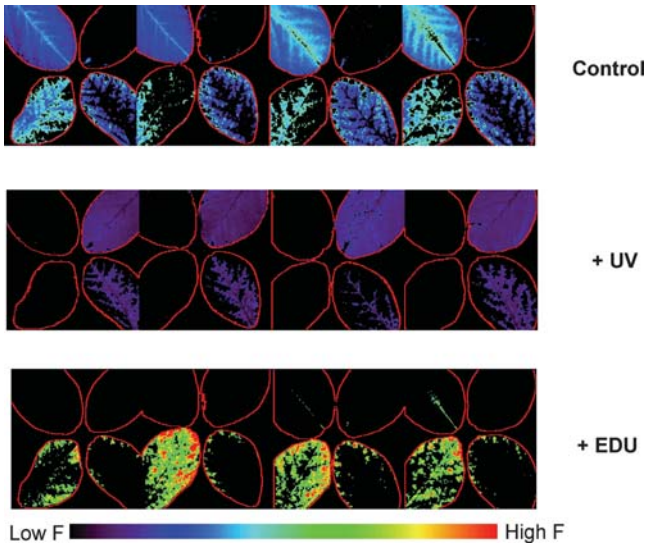

Figure 7. Regions of similarity in red_{FIS} intensity (F680) are shown for four replicates (left to right) of the FIS images shown in Fig. 5. Leaf surface areas with F emissions within the ~99 percentile from the intensity histogram per treatment are shown for the following: controls (blue), top panel; UV (purple), middle panel; and EDU (green/yellow/red), bottom panel. The colors describe the relative F intensity, as given by the color bar at the bottom, where purple indicates low F and red indicates high F.

Different trends resulted for the blue/green ratios from 380EX *vs* FIS images (Fig. 9). The $blue/green_{FIS}$ ratio strongly exhibited lower F for the UV and/or UV/EDU treatments (Fig. 9b). This was less clearly expressed by the comparable 380EX blue/green ratio, $F435/F525_{380EX}$ (Fig. 9a), which more closely resembled the pattern for the $blue/green_{280EX}$ ratio (Fig. 2d).

Dependence of fluorescence ratios on pigment content

A UV/blue 280EX ratio, $F315/F420_{280EX}$, was inversely and linearly correlated to Chl *a* content and separated the four treatment

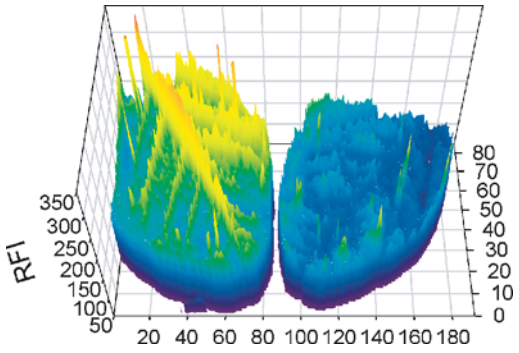

Figure 8. A 3-dimensional representation is shown for the FIS green ($green_{FIS}$, F550) image intensities for a control *vs* UV-exposed leaf. RFI, relative fluorescence intensity.

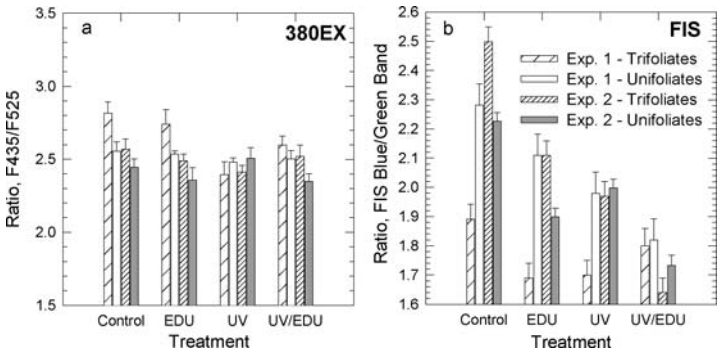

Figure 9. Bar charts show the mean ± SE for the blue/green F ratios for the 16 plant groups included in this study. These are arranged by the four treatments (control, EDU, UV and UV/EDU). Also shown are four other groups: trifoliates from Exp. 1, hatch; trifoliates from Exp. 2, dense hatch; unifoliates from Exp. 1, white; and unifoliates from Exp. 2, grey. The two blue/green ratios are from **a**] 380EX extracts and. **b**] FIS images.

groups ($R = 0.88$) when the data from the two experiments and two leaf types were combined (Fig. 10); the EDU and UV treatments had the highest and lowest ratio values, respectively. This ratio was previously reported by Middleton *et al*. (27) to correlate with total photosynthetic pigment content in a UV/EDU exposure experiment with cucumber. F420 is most likely due to emissions from polyphenolics, soluble lignin and plastoquinone (18), and also falls on the shoulder of the primary Chl *a* peak (at 435 nm) of absorbance spectra in ethanol, although shifted slightly to shorter wavelengths by the DMSO solvent (31). No 380EX variables could be related to photosynthetic pigment content. However, a dependence on total pigment content (sum of Chl *a*, Chl *b* and total carotenoids) ($R = 0.73$) was successfully demonstrated for the far-red/blue$_{FIS}$ ratio, for which separate curves resulted for each of the four treatments but with significant interactions occurring among them (not shown). Total pigment, rather than Chl *a* only, affected far-red F due to reabsorption of red F.

GLM Analysis

The GLM results are summarized in Table 3 (I. leaf characters and II. F of extracts, 280EX) and Table 4 (III. F of extracts, 380EX and IV. FIS images). Here, the relative importance of the study's various factors, especially UV-B and EDU, on measurements is evaluated based on the F values and coefficients of determination (R^2). It is revealed by the GLM that the uncontrolled experiment-to-experiment differences (Exp. 1 *vs* Exp. 2) and leaf age (unifoliates *vs* trifoliates) acted as confounding factors in determining the actual effects of the two primary factors (UV-B and EDU) on measured variables. Note that the UV-B × EDU interactions were insignificant for almost all leaf character and extract variables examined, but were common for FIS images.

For leaf characters (Table 3, section I), UV-B exposure (but not EDU uptake) was a highly significant ($P \geq 0.001$) main effect for all photosynthetic pigment variables ($R^2 \geq 0.86$) and for leaf area ($R^2 = 0.52$), and was significant ($P \geq 0.05$) for fresh leaf mass ($R^2 = 0.44$). Although UV-B did significantly increase Chl accumulation and reduce leaf area and mass, the experimental replication and leaf age were even more important contributing factors. However, EDU uptake was not a significant main effect on any leaf character. The UV × EDU interaction was nonsignificant, as were all three-factor interactions for most leaf characters.

Most 280EX and 380EX variables determined from extracts demonstrated leaf × Exp. interactions (Tables 3 and 4, sections II *vs* III). Both EDU and UV-B were highly significant ($P \geq 0.001$) main effects for two UV-A variables, F315$_{280EX}$ and F330/F385$_{280EX}$ (R^2 =0.85, 0.88). F315$_{280EX}$ was one of the few variables in the entire study not affected by interactions among factors. UV-B was also a highly significant main effect for two other UV-A/blue ratios, F330/F445$_{280EX}$ and F315/F420$_{280EX}$ ($R^2 = 0.87, 0.90$), the latter correlated to Chl *a* content (Fig. 10). The only variable in the study having EDU as the sole significant main effect was the blue/green ratio, F435/F525$_{280EX}$ ratio ($R^2 = 0.64$) (also see Fig. 2d).

The normalized red ChlF ratio, F675/F615$_{380EX}$, had highly significant UV-B and significant EDU main effects ($R^2 = 0.93$). EDU was not a significant main effect for any other 380EX variable. The ChlF peaks by themselves also exhibited UV-B main effects, but their red/far-red ratio (F675/F730$_{380EX}$) was the only variable for extracts that exhibited a significant UV × EDU interaction. Two ratios using ChlF peaks, F730/F435$_{380EX}$ and F675/F460$_{380EX}$ (Fig. 3a), also had highly significant UV-B main effects ($R^2 \sim 0.92$). For the FIS image variables (Table 4, section IV), all had two- or three-factor interactions, so that in general main effects did not emerge as primary factors influencing F, indicating their sensitivity to leaf age and uncontrolled experimental conditions.

DISCUSSION

In numerous previous studies, F measurements have proved essential for monitoring early stages of environmentally induced physiological stress (*e.g.* UV-B exposure) that is not yet manifested visually in foliage. One major thrust of our research has been to develop and evaluate the potential of F images as a remote

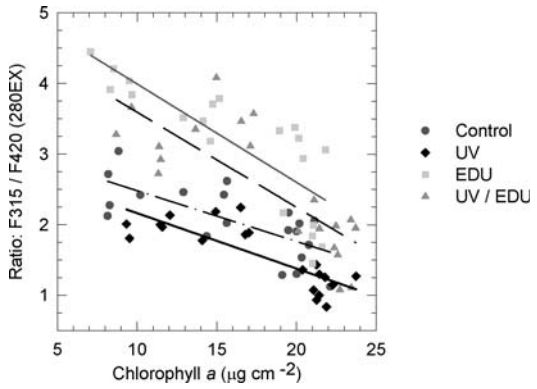

Figure 10. An F ratio was related to photosynthetic pigment content. The F315/F420$_{280EX}$ ratio was inversely and linearly dependent on Chl *a* content (µg cm^{-2}), $R^2 = 0.88$ (n = 80). Separate linear relationships are shown for the four treatments (control, dark grey circles; UV, black diamonds; EDU, light grey squares; and UV/EDU, medium grey triangles). Treatments include all available data for both leaf types and both experiments.

Table 3. GLM analysis of UV-B and EDU effects on leaf characters and flurorescence of extracts with excitation at 280 nm

			Main effects				2-Factor interactions					3-Factor interactions		
Variable	Model R^2	N	UV-B	EDU	Experiment	Leaf type	UV-B* EDU	Leaf* Exp.	UV-B* Exp.	EDU* Exp.	UV-B* Leaf	EDU* Leaf	UV-B* EDU*Exp.	UV-B* EDU*Leaf type
I. Leaf characters														
Chlorophyll *a*	0.96	80	**47.3*****	0.3ns	1363.3***	109.4***	0.4ns	**168.5*****	0.0ns	2.0ns	1.4ns	0.4ns	0.1ns	0.0ns
Chlorophyll *b*	0.96	79	**53.3*****	0.1ns	1117.0***	126.5***	1.1ns	**103.6*****	3.5ns	3.6ns	1.1ns	0.0ns	0.0ns	0.0ns
Carotenoids	0.96	79	**34.4*****	13.2***	1198.3***	32.0***	0.4ns	**97.5*****	0.0ns	**16.4*****	0.1ns	0.1ns	0.1ns	0.3ns
Chl *a*/*b*	0.86	76	**31.2*****	0.2ns	177.1***	135.5***	1.1ns	**37.9*****	0.2ns	2.0ns	2.2ns	0.2ns	3.3ns	0.3ns
Drymass	0.78	80	0.2ns	6.8**	136.4***	28.9***	1.6ns	**52.6*****	2.9ns	**8.1****	1.6ns	0.2ns	2.9ns	0.5ns
Dry SLA	0.78	77	19.1***	23.1***	60.4***	31.3***	1.4ns	**67.6*****	**9.8****	**28.7*****	2.3ns	**5.2***	0.1ns	0.1ns
Fresh mass	0.52	79	**6.1***	0.3ns	25.8***	22.4***	0.7ns	**14.5*****	0.5ns	0.1ns	0.1ns	1.2ns	0.2ns	0.7ns
Leaf area	0.44	80	**16.9*****	0.0ns	**26.0*****	**5.6***	0.4ns	0.9ns	0.0ns	0.6ns	0.3ns	1.4ns	0.3ns	0.4ns
Flavonoids (A300)	0.22	78	7.3**	0.1ns	0.0ns	0.0ns	1.2ns	0.0ns	**5.8***	0.0ns	2.9ns	0.8ns	0.0ns	0.0ns
II. Fluorescence of extracts with excitation at 280 nm														
F315/F420	0.90	80	**57.1*****	208.8***	231.9***	15.8***	1.0ns	**29.4*****	1.9ns	**22.0*****	0.1ns	**4.4***	0.2ns	0.0ns
F315	0.85	79	**48.1*****	**256.0*****	**42.9*****	**22.2*****	0.2ns	0.3ns	0.0ns	2.6ns	0.0ns	3.2ns	2.5ns	0.6ns
F330/F385	0.88	80	**79.8*****	**138.8*****	227.9***	32.6***	0.0ns	**13.5*****	2.1ns	3.3ns	0.2ns	0.5ns	0.2ns	0.0ns
F330/F445	0.87	79	**120.6*****	97.5***	139.9***	9.8***	1.5ns	**49.6*****	2.4ns	**11.8****	0.2ns	2.4ns	0.0ns	0.0ns
F330	0.77	79	109.3***	74.3***	0.1ns	19.2***	0.3ns	2.2ns	0.0ns	0.0ns	2.4ns	1.5ns	**3.8***	0.0ns
F435/F525	0.64	78	4.8*	**56.2*****	1.5ns	4.0*	1.1ns	**27.6*****	**15.2*****	1.2ns	1.2ns	0.0ns	1.2ns	0.7ns

The F values are given along with the levels of significance (***$P < 0.001$; **$P > 0.001$–0.01; *$P > 0.01$–0.05; ns, nonsignificant).
The highest order significant model terms are shown in bold type (3-factor, 2-factor, main effects).

sensing tool for this purpose (10,23,30,33), an objective also pursued by others (15–16,34–37). But most of what we know about plant F has come from studies conducted in the laboratory on excised individual leaves, leaf pieces extracted in solvents or *in situ* with contact instruments (*e.g.* ChlF kinetics). The link between that set of F measurements and those captured in F images needs to be better established. This was the rationale for evaluating FIS images in comparison with F approaches that elicit the shortwave UV-A (~330 nm) emission feature only seen when UV-B excitation wavelengths are used (*e.g.* 280EX), and the

Table 4. GLM analysis of UV-B and EDU effects on fluorescence of extracts with excitation at 380 nm and fluorescence images

			Main effects				2-Factor interactions					3-Factor interactions		
Variable	Model R^2	N	UV-B	EDU	Experiment	Leaf type	UV-B*EDU	Leaf* Exp.	UV-B* Exp.	EDU* Exp.	UV-B* Leaf	EDU* Leaf	UV-B* EDU*Exp.	UV-B* EDU*Leaf type
III. Fluorescence of extracts with excitation at 380 nm														
F675	0.93	80	**12.8*****	0.2ns	763.7***	60.6***	0.1ns	**26.8*****	0.1ns	0.0ns	0.0ns	3.2ns	0.7ns	1.9ns
F730	0.93	80	**12.7*****	0.2ns	754.9***	62.4***	0.0ns	**24.8*****	0.1ns	0.0ns	0.0ns	2.8ns	0.9ns	1.9ns
F675/F615	0.93	80	**12.4*****	4.3*	720.7***	126.0***	0.0ns	**49.5*****	0.8ns	0.3ns	1.0ns	**3.8***	0.0ns	0.4ns
F730/F615	0.93	80	**12.5*****	**4.5***	722.2***	130.8***	0.0ns	**47.2*****	0.8ns	0.4ns	0.8ns	3.3ns	0.1ns	0.4ns
F730/F525	0.94	80	19.0***	0.5ns	796.2***	106.5***	0.0ns	**47.9*****	**4.4***	0.0ns	0.0ns	0.6ns	1.4ns	0.1ns
F730/F435	0.92	80	**20.4*****	0.0ns	625.7***	95.7***	0.5ns	**26.2*****	1.9ns	2.0ns	0.5ns	0.1ns	0.8ns	1.4ns
F675/F460	0.93	80	**20.3*****	0.0ns	670.3***	89.3***	0.4ns	**35.7*****	3.0ns	0.6ns	0.4ns	0.2ns	1.0ns	0.5ns
F675/F730	0.27	80	0.1ns	0.0ns	7314.0**	0.0ns	**4.7***	**6.6***	0.0ns	1.4ns	1.8ns	1.1ns	2.1ns	0.0ns
F435	0.54	77	3.5*	0.1ns	11.8***	35.9***	0.2ns	**11.2*****	1.8ns	0.3ns	**8.8****	1.2ns	2.1ns	0.0ns
F525	0.64	73	4.7*	4.7*	0.1ns	58.8***	0.2ns	**17.1*****	**16.7*****	0.1ns	1.9ns	**4.9***	0.0ns	0.5ns
F435/F525	0.45	78	8.3**	0.1ns	14.2***	9.8**	3.0ns	0.3ns	**5.3***	1.7ns	**6.0***	2.3ns	0.6ns	3.8ns
IV. Fluorescence Images														
Blue FIS	0.87	80	288.6***	0.6ns	8.4**	33.1***	3.0ns	0.0ns	**37.0*****	8.1**	**65.2*****	0.1ns	0.3ns	0.3ns
Green FIS	0.70	75	48.3***	20.4***	1.2ns	4.5*	0.1ns	**15.9*****	8.2**	**26.7*****	**28.3*****	0.6ns	0.3ns	0.1ns
Red FIS	0.84	75	135.5***	81.9***	0.4ns	0.0ns	0.1ns	5.0*	29.0***	15.8***	31.8***	0.8ns	**50.9*****	**21.6*****
Far-red FIS	0.84	77	131.8***	73.5***	3.2ns	0.1ns	3.6ns	6.4*	23.9***	11.3**	27.0***	0.2ns	**33.5*****	**15.5*****
Far-red/blue	0.79	76	32.8***	82.4***	16.2***	7.0**	12.6***	12.5***	11.0**	5.5*	4.3ns	0.0ns	**28.8*****	**10.8****
Red/far-red	0.77	70	77.1***	43.9***	21.5***	5.1*	1.5ns	0.1ns	5.0*	5.8*	30.1**	0.7ns	3.1ns	**7.2****
Blue/green	0.72	76	58.2***	39.5***	5.9*	4.9*	2.5ns	**26.8*****	**10.7****	**13.6*****	0.1ns	0.8ns	1.3ns	2.4ns
Far-red/green	0.70	72	54.2***	24.0***	6.9**	2.1ns	9.8**	0.3ns	10.9**	1.4ns	2.4ns	0.2ns	**20.4*****	**6.4****

The F values are given along with the levels of significance (***$P < 0.001$; **$P > 0.001$–0.01; *$P > 0.01$–0.05; ns, nonsignificant).
The highest order significant model terms are shown in bold type (3-factor, 2-factor, main effects).

ChlF emissions induced by long-wave UV-A (*e.g.* 380EX) or visible wavelengths.

Interpreting FIS images and fluorescence of extracts

The FIS images were complex spatially, but the trends for averages among treatments were similar to those obtained from 280EX as shown in Fig. 2 (a–c) *vs* Fig. 6 (a–c), but did not resemble those from 380EX. This is particularly interesting because 380EX is representative of many commonly used UV-A excitation sources (*e.g.* Nd:YAG, 355 nm) associated with much of the published F vegetation findings in the last few decades. The FIS leaf images appear to be strongly influenced by the photosynthetic pigment content, especially when expressed as spectral F ratios. However, the sensitivities of the far-red/blue$_{FIS}$ ratio to total pigment load were dependent on treatment. The highest ChlF originated from leaf regions having lower total Chl, especially the leaf edges of the EDU and UV/EDU treatments as shown in Figs. 5 and 7. At the same time, UV-exposed leaves had the lowest far-red/blue$_{FIS}$ ratio, even although their total leaf Chl levels were highest. This suggests that ChlF in UV-B–exposed leaves was quenched by either the presence of UV-B–absorbing compounds or by development of thicker leaves. The latter is indicated here, because both A300 and specific leaf area were lower in UV-exposed plants (Table 2). Now we can see by examining the images (Fig. 7, middle panel, lower right leaflet per replicate) that the leaf edges of the UV/EDU were not the appropriate site for comparing pigments among treatments to obtain a general UV effect. Because this is the region where leaf discs were removed for flavonoid analyses, this may explain the inability to show increases in UV-B–absorbing compound content with UV treatment in this relatively short-term 10-day exposure study. In contrast, the F315/F420$_{280EX}$ ratio from the extracts (Fig. 10) taken from more interior sections showed a consistent, inverse response to Chl *a* content, although different curves defined the four treatments. This result appears to be rigorous, having been documented previously in cucumber leaves (10).

The FIS images, produced from a broadband UV-B and UV-A excitation, captured other F responses similar to those obtained from the 280EX, a single UV-B wavelength excitation. UV and EDU treatments both elicited the same general response pattern in the UV protein peak (Figs. 2a,b) and in the FIS ChlF bands (*e.g.* Fig. 6b): augmented F from EDU plants and reduced F from UV plants (Fig. 6; Tables 3 and 4). Whereas the FIS ChlF/blue ratios followed this pattern as well (Fig. 6c), the 380EX ChlF/blue ratio (Fig. 3a) and other 380EX ChlF variables increased primarily in response to UV-B exposures, in agreement with the UV-B–induced increase in Chl content (Table 1). Some of the F variations observed can be attributed to the following instrumentation characteristics: (1) excitation intensities and wavelengths; (2) emission band wavelength centers, band widths and sampling resolution; (3) signal-to-noise responses; and (4) integration times. For example, the 380EX ChlF emission peaks at 675 and 730 nm, determined from spectra sampled at 5 nm resolution, were slightly shifted from the slightly wider (8 nm) FIS bands centered at 680 and 740 nm.

FIS images measured F mainly from the upper foliar surfaces, but also captured F emanating from deeper tissues. However, the extracts measured F from organic compounds soluble in DMSO, including the pigments as well as proteins and the fluorescent free amino acids from cell walls, the cell matrix and the vacuoles. These compounds come from the entire vertical leaf profile, including the adaxial and abaxial surfaces and the mesophyll layers. Therefore, some of the differences observed between F responses for 380EX and FIS images are due to the influence of the contributing tissues on F intensities and properties of whole leaves *vs* extracts (27). For the spectral region common to both 280EX and 380EX emissions in the blue and green, differences in their blue/green ratios (F435/F525$_{280EX}$ *vs* F435/F525$_{380EX}$) were due to the contribution of protein emissions in the tails of the blue peaks produced by 280EX, differences in absorbance (extinction coefficients) at 280 *vs* 380 nm and/or emissions from other compounds. The blue and green F from 280EX were nearly equal across treatments, yielding a F435/F525$_{280EX}$ ratio close to 1.0 (Fig. 2d); the comparable F425/F525$_{380EX}$ ratios ranged from 1.7–2.5 across treatments (Fig. 9b).

Interpreting treatment effects

It is well known that results from UV-B exposure experiments are often difficult to replicate, because different leaf characters or plant growth variables are affected when environmental conditions vary (*e.g.* ref. 38). One reason may be that young leaves are more sensitive than older leaves to UV exposure, with new growth overtopping older leaves during the course of experiments, and partially shading the older leaves at the base of the plant. After 10 days of UV irradiation, we examined both the oldest leaf per plant that was present at the beginning and throughout the experiment as well as the youngest fully expanded leaf. The oldest, unifoliate leaves were clearly different in some intrinsic ways from young, trifoliate leaves examined; these intrinsic differences were evident because the UV-A/blue ratio (F330/F445$_{280EX}$) discriminated between the two types of leaves (Fig. 2c). This ratio most likely expresses the relative investment in structural compounds such as cell walls or starch deposition (39).

EDU was responsible for increasing the production of compounds that contributed to the elevated F of the protein peak in both young and old leaves (Fig. 2a–c). In the older unifoliate leaves, Chl content and ChlF were lower for plants provided EDU (EDU or UV/EDU, Table 1, Fig. 6) than for control plants. On the other hand, the UV treatment inhibited production of compounds contributing to the 330F peak in young and old leaves, and increased ChlF in young leaves (Fig. 3b) due to higher Chl content (Table 1). EDU uptake apparently increased the leaf investment in protective UV-A (*e.g.* 330 nm) fluorescing compounds (Fig. 2). UV-A/blue fluorescence has been shown to come from several sources, including NADPH, soluble protein tryptophanyl residues, carotenoids and precursors and cell membranes and walls (40–44). It appears that some form of competitive inhibition at the synthesis level occurred for compounds that contributed to the F330 UV-A peak *vs* those leading to Chl *a* production. This competitive inhibition may have occurred for soluble compounds sequestered in vacuoles where flavonoids are known to be concentrated, which could partially explain why flavonoid content did not increase under UV-B exposure in this experiment. This is the most likely explanation for the successful separation of UV-exposed foliage from foliage supplied EDU using blue/green$_{FIS}$ ratios (Fig. 9b). Consequently, the FIS images demonstrate the potential for use in 2-D location of appropriate sites for sample acquisitions for tissue chemical analyses, where heterogeneous leaf surface effects occur. This could provide a more powerful F-based technique, especially when combined with newer methods to measure UV-absorbing compounds with F in extracts described by Cerovic *et al.* (45).

Numerous studies have been conducted on the phytoprotective effects of EDU against ozone pollution (8,46–52). Nevertheless,

the mechanisms by which EDU confers chemical protection are still unknown and EDU can persist in the plant for 10 days or more (50). The compound has been viewed as an antiozonant by some investigators and as an antioxidant by others. Studies have shown that EDU moves systemically in plants when applied to the soil or injected into the stem (46–47, 50). Gatta *et al*. (49) have reported that it does not appear to enter cells but remains in the apoplast, suggesting that the intact molecule is involved in protection. Aside from our earlier study on cucumber (10), there have been no other reports on UV × EDU interactions. Further work is needed to elucidate the mechanisms of action of EDU in UV-irradiated plants.

CONCLUSIONS

This study demonstrates that UV-B and EDU effects on plants of a sensitive soybean cultivar can be remotely detected with F images of intact leaves, as well as by line spectral fluorescence of leaf extracts. These two stressors act differently on the plants, and their effects are manifested differently in the F characteristics. The F images we obtained are complex to interpret, but express a wealth of physiological, morphological, developmental and spatial information about leaf responses to environmental stresses. The localized within-leaf responses to the treatments shown in the F images enabled us to better elucidate the physiological effects of UV-B and EDU exposures.

Acknowledgements—The authors thank the following colleagues: J.E. McMurtrey for laboratory facilities at USDA–ARS Beltsville, MD; T. Carter for seeds (USDA–ARS, Raleigh, NC); A. Papagno (Science Systems and Applications, Inc., SSAI) for assistance with data collection and processing; and L.M. Butcher (SSAI) for assistance with graphics and technical support. This research was funded by the NASA Terrestrial Ecology Program.

REFERENCES

1. Tevini, M. (1994) Physiological changes in plants related to UV-B radiation: an overview. In *Stratospheric Ozone Depletion/UV-B Radiation in the Biosphere*, NATO ASI Series I, Vol. 18 (Edited by R. H. Biggs and M. E .B. Joiner), pp. 37–56. Springer -Verlag, Berlin, Heidelberg.
2. Burchard, P., W. Bilger and G. Weissenböck (2000) Contribution of hydroxy cinnamates and flavonoids to epidermal shielding of UV-A and UV-B radiation in developing rye primary leaves as assessed by ultraviolet-induced chlorophyll fluorescence measurements. *Plant Cell Environ*. **23**, 1373–1380.
3. Tevini, M, J. Braun and G. Fieser (1991) The protective function of the epidermal layer of rye seedlings against UV-B radiation. *Photochem. Photobiol*. **53**, 329–333.
4. Middleton, E. M. and A. H. Teramura (1993) The role of flavonol glycosides and carotenoids in protecting soybean from UV-B damage. *Plant Physiol*. **103**, 741–752.
5. Strid, A. and R. J. Porra (1992) Alterations in pigment content in leaves of *Pisum sativum* after exposure to supplementary UV-B. *Plant Cell Physiol*. **33**, 1015–1023.
6. Middleton, E. M. and A. H. Teramura (1994) Understanding responses for photosynthesis, pigments, and growth induced by UV-B and UV-A irradiances. *Photochem. Photobiol*. **60**, 38–45.
7. Lee, E. H., G. F. Kramer, R. A. Rowland and M. Agrawal (1992) Antioxidants and growth regulators counter the effects of O_2 and SO_2 in crop plants. *Agri. Ecosystem and Environ*. **38**, 99–106.
8. Kosta-Rick, R. and W. J. Manning (1993) Dose-response studies with the antiozonant ethylenediurea (EDU), applied as a soil drench to two growth substrates, on greenhouse-grown varieties of *Phaseolus vulgaris* L. *Environ. Pollution* **82**, 63–72.
9. Miller, J. E., W. A. Pursley and A. S. Heagle (1994) Effects of ethylenediurea on snap bean at a range of ozone concentrations. *J. Environ. Qual*. **23**, 1082–1089.
10. Krizek, D. T., E. M. Middleton, R. K. Sandhu and M. S. Kim (2001) Evaluating UV-B effects and EDU protection in cucumber leaves using fluorescence images and fluorescence emission spectra. *J. Plant Physiol*. **158**, 41–53.
11. Kautsky, H. (1934) Chlorophyllfluoreszenz und Kohlensäuressimilation. Das Fluoreszenzverhalten grüner Pflanzen. *Bioshemische Zeitschrift* **274**, 423–434.
12. Papageorgiou, G. (1975) Chlorophyll fluorescence: an intrinsic probe of photosynthesis. In *Bioenergetics of Photosynthesis* (Edited by Govindjee), pp. 320–371. Academic Press, New York.
13. Snel, J. F. H. and O. Van Kooten (1990) The use of chlorophyll fluorescence and other non-invasive spectroscopic techniques in plant stress physiology. *Photosynth. Res*. **25**, 146–332.
14. Mohammed, G. H., W. D. Binder and S. L. Gillies (1995) Chlorophyll fluorescence: a review of its practical forestry applications and instrumentation. *Scand. J. For. Res*. **10**, 383–410.
15. Lang, M., H. K. Lichtenthaler, M. Sowinska, F. Heisel and J. A. Miehé (1996) Fluorescence imaging of water and temperature stress in plant leaves. *J. Plant Physiol*. **148**, 613–621.
16. Lichtenthaler, H. K. and J. A. Miehé (1997) Fluorescence imaging as a diagnostic tool for plant stress. *Trends Plant Sci*. **2**, 316–320.
17. Kim, M. S., J. E. McMurtrey, C. L. Mulchi, C. S. T. Daughtry, E. W. Chappelle and Y. R. Chen (2001) Steady state multispectral fluorescence imaging system for plant leaves. *Appl. Optics* **40**, 157–166.
18. Chappelle, E., F. Wood, J. McMurtrey and W. Newcomb (1984) Laser-induced fluorescence of green plants. 1: a technique for the remote detection of plant stress and species differentiation. *Appl. Optics* **23**, 134–138.
19. Lichtenthaler, H. K. and U. Rinderle (1988) The role of chlorophyll fluorescence in the detection of stress conditions in plants. *CRC Press Critical Reviews in Analytical Chemistry* **19**(Suppl. 1), 29–85.
20. McMurtrey, J. E., E. W. Chappelle, M. S. Kim, J. J. Meisinger and L. A. Corp (1994) Distinguishing nitrogen fertilization levels infield corn (*Zea mays* L.) with actively induced fluorescence and passive reflectance measurements. *Remote Sens. of Environ*. **47**, 36–44.
21. Cerovic, Z. G., G. Samson, F. Morales, N. Tremblay and I. Moya (1999) Ultraviolet-induced fluorescence for plant monitoring: present state and prospects. *Agronomie* **19**, 543–578.
22. Agati, G., Z. G. Cerovic and I. Moya (2000) The effect of decreasing temperature up to chilling values on the *in vivo* F685/F735 chlorophyll fluorescence ratio in *Phaseolus vulgaris* and *Pisum sativum*: The role of the Photosystem I contribution to the 735 nm fluorescence band. *Photochem. Photobiol*. **72**, 75–84.
23. Corp, L. A., J. E. McMurtry, E. M. Middleton, C. L. Mulchi, E. W. Chappelle and C. S. T. Daughtry (2003) Fluorescence sensing systems: *in vivo* detection of biophysical variations in field corn due to nitrogen supply. *Remote Sens. of Environ*. **86**, 470–479.
24. Kim, M. S., C. L. Mulchi, C. S. T. Daughtry and J. E. McMurtrey (2003) Assessment of combined effects of elevated tropospheric O_3 and CO_2 on soybean under well-watered and restricted soil moisture conditions by multispectral fluorescence imaging techniques. *ASA Special Publication* **66**, 223–253.
25. Tevini, M., P. Grusemann and G. Fieser (1988) Assessment of UV-B stress by chlorophyll fluorescence analysis. In *Applications of Chlorophyll Fluorescence in Photosynthesis Research, Stress Physiology, Hydrobiology, and Remote Sensing* (Edited by H. K. Lichtenthaler), pp. 229–238. Kluwer Academic Press Publishers, Dordrecht.
26. Subhash, N., P. Mazzinghi, G. Agati, F. Fusi and B. Lercari (1995) Analysis of laser-induced fluorescence line shape of intact leaves: application to UV stress detection. *Photochem. Photobiol*. **62**, 711–718.
27. Middleton, E. M., E. W. Chappelle, T. Cannon, P. Adamse and S. Britz (1996) Initial assessment of physiological response to UV-B radiation using fluorescence measurements. *J. Plant Physiol*. **148**, 68–77.
28. Larsson, E. H., J. F. Bornman and H. Asp (1998) Influence of UV-B irradiation and Cd^{2+} on chlorophyll fluorescence, growth, and nutrient content in *Brassica napus*. *J. Exp. Bot*. **49**, 1031–1039.
29. Silvius, J. E., D. F. Kramer and D. R. Lee (1978) Carbon assimilation and translocation in soybean leaves at different stages of development. *Plant Physiol*. **62**, 54–58.

30. Kim, M. S., D. T. Krizek, C. S. T. Daughtry, J. E. McMurtrey, R. Sandhu, E. W. Chappelle, L. A. Corp and E. M. Middleton (1997) Fluorescence imaging system: Application for the assessment of vegetation stresses. In: Remote Sensing of Vegetation and Sea (Edited by G. Cecchi, G. D'Urso, E. T. Engman, and P. Gudmandsen), Proc. SPIE 2959, pp. 4–13.
31. Wellburn, A. (1994) The spectral determination of chlorophylls a and b, as well as total carotenoids using various solvents with spectrophotometers of different resolution. *J. Plant Physiol.,* **144**, 307–313.
32. Barnes, J. D., L. Balaguer, E. Manrique, S. Elvira, and A. W. Davison (1992) A reappraisal of the use of DMSO for the extraction and determination of chlorophylls *a* and *b* in lichens and higher plants. *Environ. Exp. Bot.* **32**, 85–100.
33. Kim, M. S., C. L. Mulchi, C. S. T. Daughtry and J. E. McMurtrey (2003). Assessment of combined effects of elevated tropospheric O_3 and CO_2 on soybean under well-watered and restricted soil moisture conditions by multispectral fluorescence imaging techniques. *Crop Physiol.* **66**, 223–253.
34. Lichtenthaler, H. K., M. Lang, M. Sowinka, F. Heisel and J.A. Miehé (1996) Detection of vegetation stress via new high resolution fluorescence system. *J. Plant Physiol.* **148**, 599–612.
35. Buschmann, C. and H. K. Lichtenthaler (1998) Principles and characteristics of multi-colour fluorescence imaging of plants. *J. Plant Physiol.* **152**, 297–314.
36. Buschmann, C. G. Langsdorf and H. K. Lichtenthaler (2000) Imaging of blue, green, and red fluorescence emission of plants: An overview. *Photosynthetica* **38**, 483–491.
37. Ounis, A., Z. Cerovic, J. Briantais and I. Moya (2001) Dual-Ex FLIDAR for the estimation of epidermal UV absorption in leaves and canopies. *Remote Sens. of Environ.* **76**, 33–48.
38. Krizek, D. T., R. M. Mirecki and G. F. Kramer (1994) Growth analysis of UV-B irradiated cucumber seedlings as influenced by photosynthetic photon flux source and cultivar. *Physiol. Plant.* **90**, 593–599.
39. Britz, S. J. and P. Adamse (1994) UV-B-induced increase in specific leaf weight of cucumber as a consequence of increased starch content. *Photochem. Photobiol.* **64**, 116–119.
40. Fujimori, E. (1981). Blue fluorescence and crosslinking of photo-oxidized proteins. *FEBS Letters* **135**, 257–260.
41. Caldwell, C. R. (1987) Temperature-induced protein conformational changes in barley root plasma membrane-enriched microsomes, II. intrinsic protein fluorescence. *Plant Physiol.* **84**, 924–929.
42. Caldwell, C. R. (1993) Ultraviolet-induced photodegradation of cucumber (*Cucumis sativus* L.) microsomal and soluble protein tryptophanyl residues in vitro. *Plant Physiol.* **101**, 947–953.
43. Cerovic, Z. G., M. Bergher, Y. Goulas, S. Tosti and I. Moya (1993) Simultaneous measurement of changes in red and blue fluorescence in illuminated isolated chloroplasts and leaf pieces: the contribution of NADPH to the blue fluorescence signal. *Photosynthesis Res.* **36**, 193–204.
44. Lang, M., P. Siffel, Z. Braunova and H. K. Lichtenthaler (1992) Investigations of the blue-green fluorescence emission of plant leaves. *Plant Cell Environ.* **15**, 91–98.
45. Cerovic, Z. G., A. Ounis, A. Cartelat, G. Latouche, Y. Goulas, S. Meyer and I. Moya (2002) The use of chlorophyll fluorescence excitation spectra for the non-destructive *in situ* assessment of UV-absorbing compounds in leaves. *Plant, Cell, and Environ.* **25**, 1663–1676.
46. Bennett, J. H., E. H. Lee and H. H. Heggestad (1978) Apparent photosynthesis and leaf stomatal diffusion in EDU treated ozone-sensitive bean plants. In *Proc. Plant Growth Regulator Working Group 5th Ann. Meet.*, pp.242–246, Virginia Polytechnic Institute and State University, Blacksburg, VA.
47. Bortier, K., G. Dekelever, L. De Temmerman and R. Ceulemans (2001) Stem injection of *Populus nigra* with EDU to study ozone effects under field conditions. *Environ. Pollut.* **111**, 199–208.
48. Carnahan, J. E., E. L. Jenner and E. K. W. Wat. (1978) Prevention of ozone injury to plants by a new protectant chemical. *Phytopathology* **68**, 1225–1229.
49. Gatta, L., L. Mancino and R. Frederico (1997) Translocation and persistence of EDU (ethylenediurea) in plants: the relationship with its role in ozone damage. *Environ. Pollut.* **96**, 445–448.
50. Godzik, B. and W. J. Manning (1998) Relative effectiveness of ethylene-diurea, and constituent amounts of urea and phenylurea in prevention of ozone injury to tobacco. *Environ. Pollut.* **111**, 199–208.
51. Manning, W. J., R. B. Flagler and M. A. Frenkel (2003) Assessing plant response to ambient ozone: growth of ozone-sensitive loblolly pine seedlings treated with ethylenediurea or sodium erythorbate. *Environ. Pollut.* **126**, 73–81.
52. Roberts, B. R., L. R. Wilson, J. J. Cascino and G. P. Smith (1987) Autoradiographic studies of ethylenediurea distribution in woody plants. *Environ. Pollut.* **45**, 81–86.